Crashworthiness Characteristics of Thin-Walled Multi-Cell Structures via the Application of Annealing Process: An Experimental Investigation

Hidayat, Dony
Department of Mechanical, Faculty of Engineering, Universitas Indonesia

Istiyanto, Jos
Department of Mechanical, Faculty of Engineering, Universitas Indonesia

Danardono Agus Sumarsono
Department of Mechanical, Faculty of Engineering, Universitas Indonesia

Kurniawan, Farohaji
Research Center for Aeronautics Technology, The National Research and Innovation Agency (BRIN)

他

https://doi.org/10.5109/7236840

出版情報：Evergreen. 11 (3), pp.1892-1900, 2024-09. 九州大学グリーンテクノロジー研究教育センター
バージョン：

Crashworthiness Characteristics of Thin-Walled Multi-Cell Structures via the Application of Annealing Process: An Experimental Investigation

Dony Hidayat[1,2,*], Jos Istiyanto[1], Danardono Agus Sumarsono[1,*], Farohaji Kurniawan[2], Kosim Abdurohman[2]

[1]Department of Mechanical, Faculty of Engineering, Universitas Indonesia, Depok, Indonesia

[2]Research Center for Aeronautics Technology, The National Research and Innovation Agency (BRIN), Bogor, Indonesia

E-mail: dony.hidayat@brin.go.id; danardon@eng.ui.ac.id

(Received January 11, 2024: Revised June 10, 2024: Accepted July 9, 2024).

Abstract: The present research aims to evaluate the initial crashworthiness characteristics of resin-coated 3D-printed Thin-Walled Multi-Cell Structures (TWMCS) are affected by annealing parameters, specifically temperature and time, during quasi-static compression. The optimal parameter combination, determined through the Signal-to-Noise (S/N) ratio and analyzed using Analysis of Variance (ANOVA), identified key factors that have a substantial impact on the crashworthiness performance. Resin coating applied to TWMCS polymer tubes results in a substantial increase in Specific Energy Absorption (SEA) values, exhibiting a 41% improvement compared to tubes without resin coating. Optimal annealing conditions for SEA were found to be 80°C for 40 minutes, and the optimal conditions for achieving maximum Crushing Force Efficiency (CFE) were determined to be at a temperature of 80°C for 70 minutes. The combined application of resin coating and annealing leads to a 57% increase in SEA compared to specimens without either treatment. This study identifies new prospects for improving TWMCS with higher energy absorption capabilities. These improvements have the potential to enhance passenger safety and strengthen the infrastructure of transportation.

Keywords: Crashworthiness; Thin-Walled Multi-Cell Structures (TWMCS); Additive Manufacturing (AM); Resin Coating; Annealing; Optimization

1. Introduction

Energy absorbers constructed from TWMCS are extensively employed in the realm of protective systems to efficiently dissipate kinetic energy through the plastic deformation process, thereby enhancing the crashworthiness of these systems. Numerous researchers have conducted studies with the primary objective of augmenting the energy absorption capabilities of TWMCS. These efforts involve the utilization of various materials such as metallic materials[1,2], fiber-reinforced composite[3], polymer[4,5], and hybrid[6–8]. The analytical methods employed encompass theoretical analysis[9], numerical modeling[10], and experimental testing[11].

In recent times, composite and polymer materials have garnered significant interest owing to their exceptional mechanical characteristics and impressive lightweight attributes[12]. Hence, numerous researchers have employed composite and polymer materials in fabricating energy-absorbing structures to enhance crashworthiness and reduce weight[12–14]. One of the manufacturing methods that utilizes composite and polymer materials is AM.

Fused deposition modeling (FDM) or 3D printing is among the AM methods capable of producing objects with diverse shapes and geometries, particularly those encompassing intricate design elements that are unfeasible to fabricate using conventional methods[15]. Lately, the combination of various elements has resulted in a tremendous surge in the utilization of FDM, largely driven by significant advancements in the consumer segment, especially in the field of economical thermoplastic extrusion FDM[16,17]. Given the widespread applications in various industries, there arises a need for a comprehensive mechanical assessment of the produced printed components[18].

While FDM presents numerous unique advantages compared to conventional manufacturing techniques, it still encounters challenges and obstacles. This is due to the layer-by-layer fabrication approach employed in FDM, resulting in produced parts exhibiting anisotropic properties because of interlayer bonding deficiencies and the alignment of pathways within layers[19]. To mitigate

these adverse effects, post-treatment is essential following the 3D printing manufacturing process.

Post-processing techniques can be categorized into two main groups: mechanical techniques, including machining, polishing, and sanding; and chemical techniques, encompassing processes such as annealing[20], remelting[21], and coating[22–24]. Yang et al.[25] explored the impact of resin coating on the mechanical characteristics and ballistic efficacy of prepreg fabric designed for armor-grade applications. Applying resin coating, adept at filling inter-filament voids without inducing resin excess, has enhanced both tensile stress and ballistic energy absorption properties.

Annealing has been extensively researched in recent years as a method to improve the mechanical properties of PLA (Poly Lactic Acid)[26,27]. As mentioned previously, annealing aims to enhance PLA's crystallinity, thereby improving its mechanical properties. When subjected to heat, the application of thermal energy serves to fill the inter-layer spaces, consequently yielding a more refined surface. The reduction in viscosity at the glass transition temperature leads to the minimization of molecular surface tension, facilitating material flow across the surface. This reflow process effectively addresses porous regions, inter-layer gaps, and the staircase effect, thereby culminating in an enhanced surface finish and improved mechanical properties[28]. The annealing of the samples resulted in enhanced material strength, with an approximately 11-17% increase in flexural stress, while no notable alteration in the modulus was observed [29]. Bhandari et al.[30] analyzed the effects of annealing at an optimal temperature, the interlayer tensile strength of the PLA-CF (Carbon fiber), resulting in a twofold increase compared to samples without annealing.

Design of Experiments (DOE) methodologies have become invaluable tools for evaluating the influence of various design parameters on product quality and reliability, and can also be employed to optimize annealing parameters. Widely employed DOE methods include factorial designs, the Taguchi approach[31], and response surface methodology (RSM)[32]. ANOVA remains the most common statistical technique for processing test results. However, the rapidly developing field of copula[33,34] theory offers an alternative approach for analyzing complex dependencies within datasets. The Taguchi method, in particularly, excels in efficiency, noise reduction, and robust design. It reduces the number of experiments required, minimizes the impact of noise factors, and achieves designs that are less sensitive to variations, thereby optimizing product and process performance[35].

This study aims to optimize the annealing parameters to enhance the crashworthiness performance of PLA TWMCS treated with resin coating. The annealing parameters varied temperatures at levels of 90°C, 120°C, and 160°C, and annealing times at levels of 30, 60, and 120 minutes. The Taguchi approach will be employed to analyze the data, while ANOVA techniques will be utilized to identify significant factors and assess their impact on crashworthiness performance. This research is expected to yield valuable insights for improving the crashworthiness of 3D-printed structures, thereby advancing knowledge in this domain and potentially enhancing passenger safety and strengthening the transportation infrastructure.

2. Experimental Section

2.1 The filament

In this study, PLA filament was purchased from eSUN. The unprocessed filament had a standard diameter of 1.75 mm and was introduced into a nozzle through a roller system. Subsequently, a nozzle with a diameter of 0.8 mm was used to extrude the melted filament. The density, tensile strength, and flexural strength of PLA are 1.23 g/cm^3, 63 MPa, and 74 MPa, respectively[11].

2.2 The preparation of specimens

The experimental specimens in the study shared consistent characteristics, with a uniform thickness of 1 mm on the tube wall and the multi-cell structure. Additionally, all specimens were standardized to a height of 50 mm. The distinguishing feature of the multi-cell structures was their 25 mm diameter, denoted as 'D.' To provide a visual representation, a Computer-Aided Design (CAD) model of the multi-cell specimen can be observed in Fig. 1. In the manufacturing specimens, PLA samples are meticulously produced using a Creality 3D printer, with each layer of the specimen being meticulously crafted in the vertical (z) dimension. These specimens maintain a consistent layer height of 0.1 mm, employ a 100% infill density, and utilize a lines infill pattern. The build plate is maintained at a temperature of 60°C, while the nozzle operates at a controlled temperature of 210°C. All other parameters of the Creality 3D printer are maintained at their default settings.

2.3 Experimental methods

Taguchi extended the principles of fractional factorials by employing orthogonal arrays for evaluating the quality of experimental outcomes[36]. He advocated for the adoption of orthogonal arrays and signal-to-noise (S/N) ratios as valuable tools for designers aiming to establish a resilient methodology less vulnerable to interference. The signal-to-noise ratio (S/N ratio) is classified into three distinct groups, each aligned with specific desired outcomes: maximization, minimization, and nominal better[35].

The annealing process was applied to thin-walled multi-cell tube specimens made of PLA using an oven, with time variations set at 30 minutes, 60 minutes, and 120 minutes, along with temperature variations of 90°C, 120°C, and 160°C (refer to Table 1). The data obtained from the heat-treated specimens were then compared to those without

heat treatment to assess the increase in strength resulting from this treatment.

Table 1. Parameters and levels for specimens.

Parameter	Level		
	1	2	3
Temperature (°C)	90	120	160
Times (minutes)	30	60	120

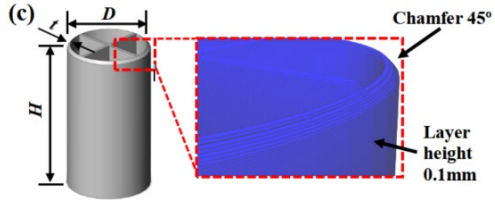

Fig. 1: Specimen dimensions.

To investigate the impact of coating and annealing, we employed a thin-walled multi-cell tube specimen made of PLA material. Subsequently, the polymer tube was coated with epoxy resin, as illustrated in Fig. 2. The resin curing process took 5 hours, followed by a heat treatment (annealing) process.

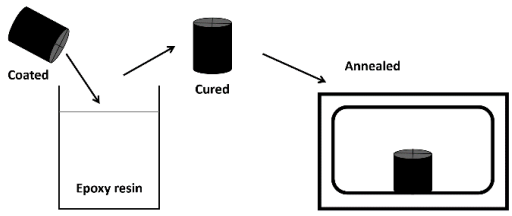

Fig. 2: Phases in the coating and annealing procedure.

A Taguchi approach was employed to optimize the crashworthiness performance of thin-walled multi-cell polymer tubes undergoing resin coating and heat treatment. In conducting the experiments, two distinct input parameters were chosen, each with three levels of variables, as outlined in Table 1. The experimental method utilized a Taguchi orthogonal array with an L9 configuration (Fig. 3).

To enhance crashworthiness performance, we applied the "bigger is better" principle, as defined by Equation (1), to illustrate the corresponding response.

$$\frac{S}{N} = -10\log\left(\frac{1}{n}\sum_{i=1}^{n}\frac{1}{y_i^2}\right) \quad (1)$$

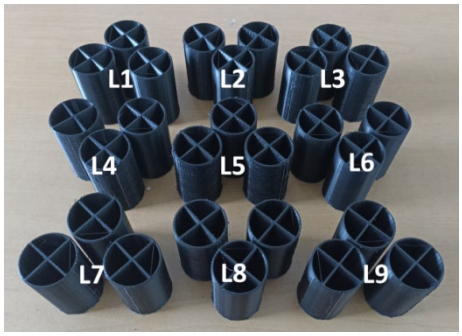

Fig. 3: Thin-walled multi-cell tube specimens subjected to resin coating and annealing treatment.

2.4 Crashworthiness Characteristics

The experimental setup used to evaluate the crashworthiness characteristics of resin-coated and annealed PLA structures was investigated by axial quasi-static compressive tests utilizing a Tensilon universal mechanical testing machine. The crosshead speed used was 5 mm/min with a maximum crushing displacement of 2/3 of the initial total height.

Several criteria are commonly employed to evaluate crashworthiness, including energy absorption (EA), specific energy absorption (SEA), mean crushing force (MCF), peak crushing force (PCF), and crush force efficiency (CFE)[37]. EA denotes the total energy absorbed by the structure while undergoing the crushing process, determined by computing the area beneath the force-displacement curve, as illustrated in Equation (2).

$$EA = \int_0^d F(x)dx \quad (2)$$

F(x) denotes the crushing load, and *d* is the relevant crushing distance. SEA signifies the energy absorbed per unit mass of the structure, which serves as an important indicator of the structure's ability to absorb energy. Mathematically, this is expressed in Equation (3).

$$SEA = \frac{EA}{m} \quad (3)$$

The average crushing force throughout the crushing process is known as MCF, and it may be expressed in Equation (4).

$$MCF = \frac{EA}{d} \quad (4)$$

In Equation 5, CFE is defined as the ratio of MCF to PCF. A higher CFE value indicates superior performance of the energy-absorbing structure.

$$CFE = \frac{MCF}{PCF} \quad (5)$$

2.5 Determination of optimal treatments

In this study, the ANOVA method is utilized to examine the impact of various factors on output parameters. This

statistical tool aids in assessing the effects of different factors on process outcomes by investigating mean squares and errors at an individual level[38]. Prior to conducting the ANOVA, the Anderson-Darling tests were employed to assess the normality of SEA and CFE data. Subsequently, a regression analysis was performed to identify the best-fitting model that relates the annealing temperature and time to the dependent variables (SEA and CFE).

3. Result and Discussion

The application of resin coating not only enhances aesthetic appearance and provides protection against environmental conditions but also significantly influences the structural strength of components produced through the 3D printing method. This study sought to leverage the benefits of resin coating on thin-walled multi-cell polymer tubes manufactured using 3D printing. Following the molding process, resin was applied as a coating using the immersion method.

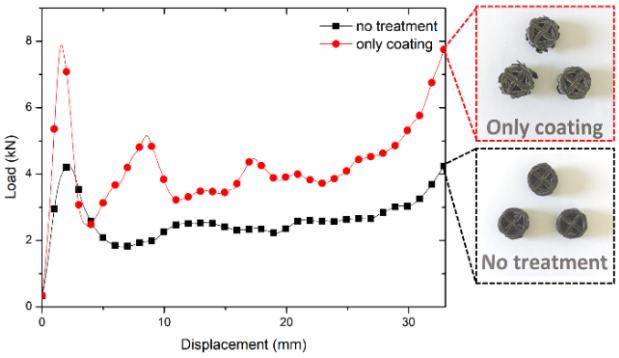

Fig. 4: The Force-displacement curve of coated and uncoated tubes.

To assess the crashworthiness performance of the tube, quasi-static testing was conducted, and a force-displacement graph was generated, as illustrated in Fig. 4. The graph reveals a 41% increase in SEA for the resin-coated tube compared to its uncoated counterpart. Furthermore, the slope of the elastic region before reaching the peak force is more pronounced in the resin-coated specimen, indicating an augmentation in the stiffness of the resin-coated tube. Applying resin coating, adept at filling inter-layer voids without inducing resin excess, has enhanced both tensile stress and energy absorption properties[25]. The resin coating acts as a reinforcing layer, distributing stress more evenly throughout the PLA structure, reducing stress concentrations, and preventing premature failure.

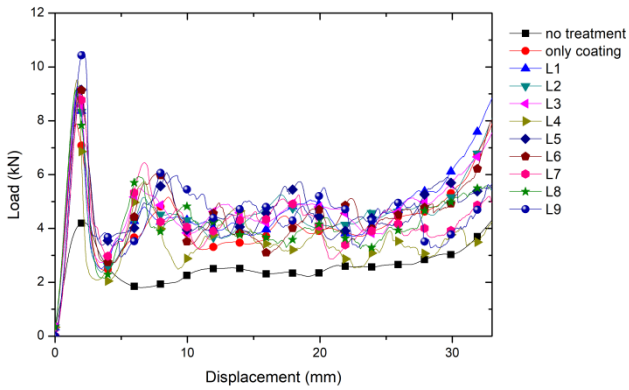

Fig. 5: Force-displacement graphs for coated and annealed thin-walled multi-cell tubes.

The peak force values of specimens subjected to resin coating and heat treatment (annealing) exhibit a significant increase compared to untreated specimens. The annealing process effectively addresses porous regions, inter-layer gaps, and the staircase effect, thereby culminating in an enhanced surface finish and improved mechanical properties[28]. Nevertheless, following the peak force, all specimens experience a notable decrease in load-bearing capacity to approximately 2 - 3 kN, as illustrated in Fig. 5. After the initial fold, observed by the formation of the initial peak in the graph, untreated specimens form the subsequent fold with a force around 2 - 2.5 kN and tend to stabilize. In contrast, specimens with resin coating and heat treatment display a fluctuating graph after the initial peak force. The folds formed in these specimens are accompanied by fragmentation, evident on the graph as a sudden, dramatic drop in force when fragmentation occurs in the specimen.

Table 2. Experimental findings of the crashworthiness performance of multi-cell tubes that have undergone resin coating and heat treatment.

Experiment Number	Parameter		SEA (J/gr)	CFE
	Temperature (ºC)	Time (minutes)		
L1	80	30	17.53	0.54
L2	80	60	17.04	0.52
L3	80	120	17.51	0.54
L4	120	30	12.96	0.39
L5	120	60	16.68	0.51
L6	120	120	16.92	0.52
L7	160	30	15.40	0.48
L8	160	60	15.36	0.48
L9	160	120	16.10	0.43

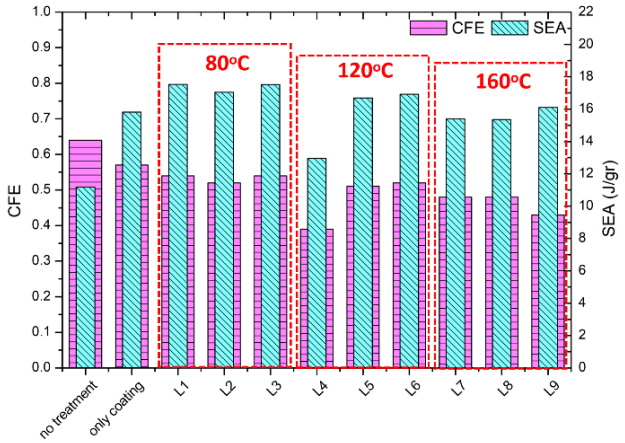

Fig. 6: The crashworthiness performance of heat-treated specimens.

Figure 6 depicts the crashworthiness performance (SEA and CFE) of thin-walled multi-cell polymer tubes subjected to resin coating and heat treatment. The SEA value of the specimens shows a considerable increase (41%) after the application of resin coating, while the CFE value decreases by 12%. This is attributed to a substantial increase in strength and stiffness (Fig. 5), resulting in a significant rise in peak crushing strength (87%). However, the average crushing strength only experiences a 65% increase.

Verifying model assumptions before DOE analysis is crucial, as violations can compromise the validity of derived conclusions. Consequently, diagnostic plots were meticulously examined to identify any potential deviations from the assumed underlying data structure. As depicted in Fig. 7, the plot visually confirms a pattern consistent with a normal distribution of errors for SEA.

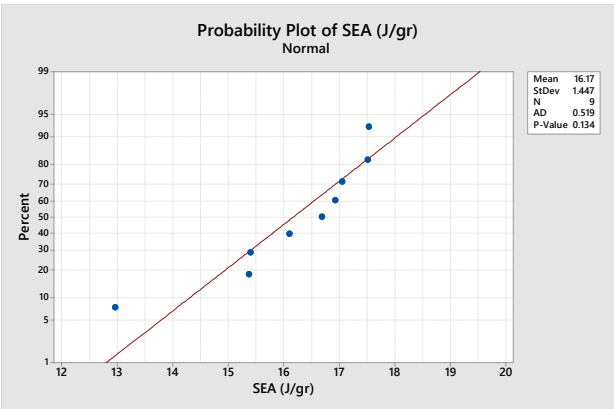

Fig. 7: Probability plot for SEA

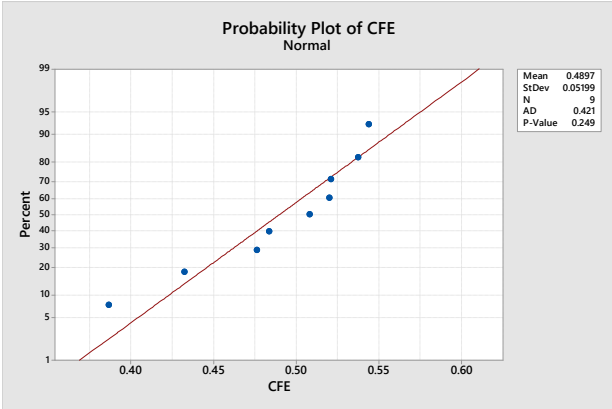

Fig. 8: Probability plot for CFE

Figure 8 depicts the graphical representation of the CFE's normal probability, as derived from the modelling process. This graph assesses the accuracy of the model. With P-values exceeding 0.05 on the normality graph and residuals adhering to a normal distribution, it indicates compatibility between the experimental study and the mathematical model. Moreover, the proximity of the distribution to the central axis signifies the balanced and accurate nature of the experimental model.

The SEA values also increase when tubes coated with resin undergo heat treatment, as observed in Fig. 6. The highest increase in SEA occurs at the 80°C heat treatment, with an 11% enhancement for treatment durations of 30 and 120 minutes. Fig. 9 illustrates the signal-to-noise (S/N) ratio for SEA values in thin-walled multi-cell polymer tubes influenced by temperature and heat treatment duration parameters. The analysis of temperature's influence on SEA values in the experiment reveals the highest S/N ratio at 80°C, reaching 24.75. Meanwhile, the impact of heat treatment duration shows its peak value at 120 minutes.

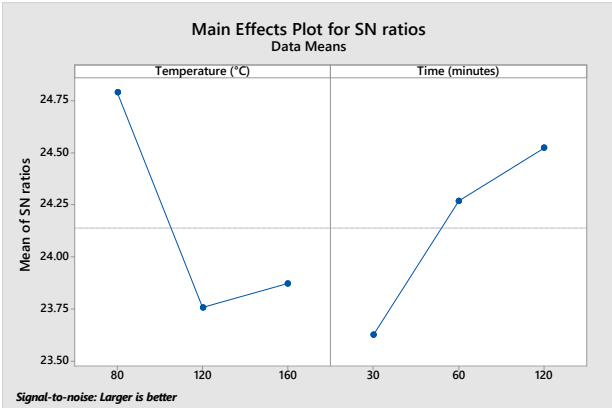

Fig. 9: The mean SN ratio for SEA in resin-coated and annealed tubes.

Figure 10 depicts the signal-to-noise (S/N) ratio for CFE values in thin-walled multi-cell tubes influenced by temperature and heat treatment duration parameters. Analysis of the temperature's impact on CFE values in the experiment reveals the highest S/N ratio, reaching -5.50 at

a temperature of 80°C. Meanwhile, the highest value for heat treatment duration occurs at 60 minutes. To achieve thin-walled multi-cell polymer tubes with maximum CFE values, resin coating and heat treatment at 80°C for 60 minutes are required.

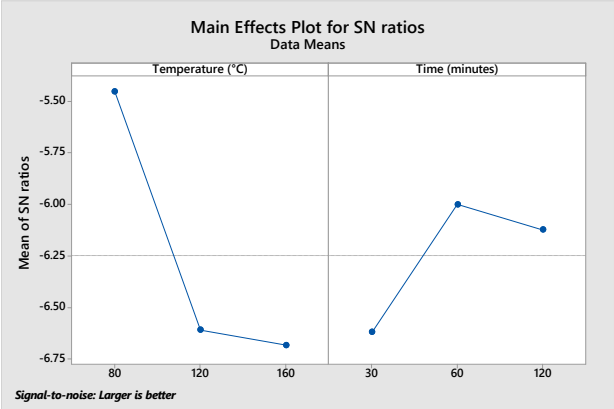

Fig. 10: The mean SN ratio for CFE in resin-coated and annealed tubes.

To enhance the crashworthiness performance of TWMCS, this study investigates the influence of annealing variables, particularly temperature and time. These variables are known to impact SEA and CFE values significantly. The ANOVA analysis for SEA values (Table 3) revealed that temperature (38.21%) and time (22.44%) were the significant contributing factors. Similarly, for CFE values (Table 4), temperature (41.16%) exerted a more significant influence compared to time (7.29%).

Table 3. Analysis of variance of SEA

Source	Contribution	Adj SS	Adj MS	p-value
Temperature (°C)	38.21%	6.405	3.202	0.257
Time (minutes)	22.44%	3.761	1.880	0.406
Error	39.35%	6.594	1.649	
Total	100.00%			

Table 4. Analysis of variance of CFE

Source	Contribution	Adj SS	Adj MS	p-value
Temperature (°C)	41.16%	0.008	0.004	0.309
Time (minutes)	7.29%	0.002	0.001	0.767
Error	51.55%	0.011	0.003	
Total	100.00%			

The experiment yielded results by differentiating multiple parameters (temperature and time). These results were utilized to develop regression equations. A suitable mathematical model was constructed for each output response, such as SEA and CFE. Regression analysis was used to analyze the SEA, and Equation (6) presents the best fit for SEA. The regression analysis is employed for the CFE, and Equation (7) presents the best fit for CFE.

$$\text{SEA (J/gr)} = 16.167 + 1.192\ \text{Temperature (°C)\_80} - 0.644\ \text{Temperature (°C)\_120} - 0.547\ \text{Temperature (°C)\_160} - 0.871\ \text{Time (minutes)\_30} + 0.195\ \text{Time (minutes)\_60} + 0.676\ \text{Time (minutes)\_120} \quad (6)$$

$$\text{CFE} = 0.4897 + 0.0443\ \text{Temperature (°C)\_80} - 0.0184\ \text{Temperature (°C)\_120} - 0.0259\ \text{Temperature (°C)\_160} - 0.0185\ \text{Time (minutes)\_30} + 0.0118\ \text{Time (minutes)\_60} + 0.0066\ \text{Time (minutes)\_120} \quad (7)$$

Surface plots illustrating SEA values over time and temperature variations for resin-coated thin-walled multi-cell polymer tubes are presented in Fig. 11. Achieving SEA values exceeding 18 J/gr is accomplished through an anneal treatment temperature of 80°C, while the anneal treatment duration ranges from 40 to 120 minutes. The observed increase in SEA value for resin-coated specimens post-heat treatment is 11%, compared to specimens without heat treatment.

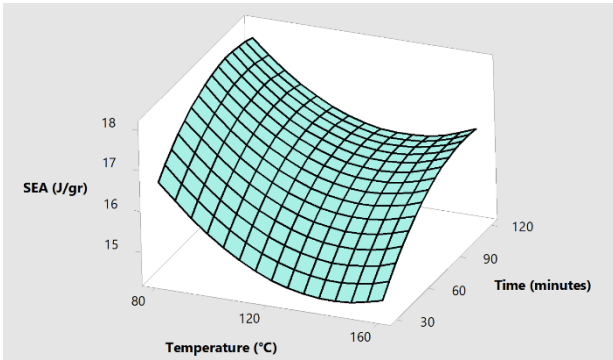

Fig. 11: Surface plot of SEA (J/gr)

Surface plots illustrating the CFE values concerning variations in time and temperature for thin-walled, resin-coated, multi-cell polymer tubes are depicted in Fig12. The findings indicate that achieving CFE values exceeding 0.55 requires heat treatment at 80°C, with treatment durations ranging from 70 to 120 minutes. The resin coating process applied to the thin-walled multi-cell polymer tubes significantly enhanced their strength and stiffness, substantially increasing peak crushing strength by 87%. However, the average crushing strength exhibited a more moderate rise of 65%. Consequently, the average CFE of the resin-coated and heat-treated tubes experienced a reduction of approximately 14%.

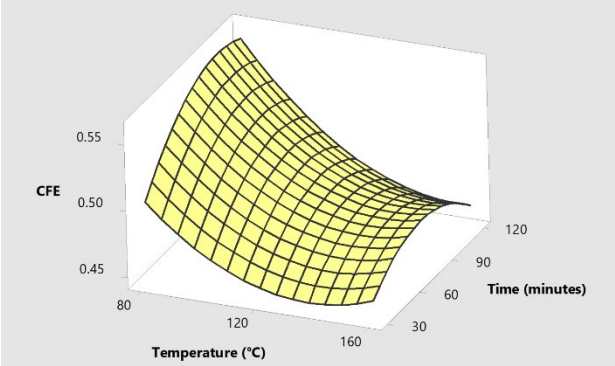

Fig. 12: Surface plot of CFE

Among the nine variations of annealing applied to thin-walled multi-cell polymer tubes, those designated as L3 exhibited the highest SEA and CFE values, as presented in Table 2. To elucidate the failure mode of these tubes and compare them with their untreated, resin-coated, and heat-treated counterparts, we combined the load-to-displacement data with the tubes' post-testing appearance, as illustrated in Fig. 13.

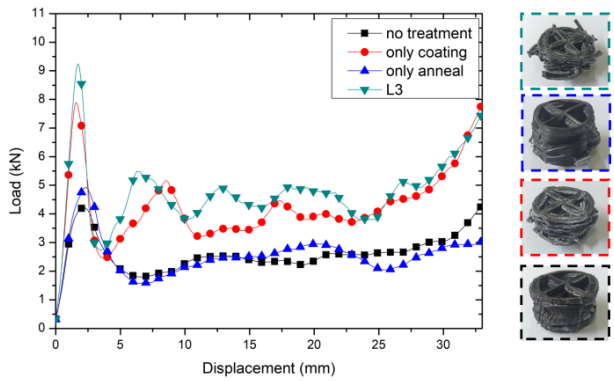

Fig. 13: The Force-displacement curve thin-walled multi-cell polymer tubes with various treatment conditions.

Thin-walled multi-cell polymer tubes subjected solely to heat treatment exhibited a 17% increase in initial peak force. In contrast, the application of resin coating to the thin-walled multi-cell tubes not only enhanced initial peak force but also stiffness, as evident in Fig. 13. A discernible change in the graph's slope before reaching the initial peak force is observed in the resin-coated tube. The reinforcing effect of resin coating resulted in a 41% increase in SEA value, while heat treatment alone led to an 11% increase, mirroring the findings of the tubes treated solely with heat.

The untreated tubes exhibited folding in a buckling mode with some delamination observed on the tube wall. In contrast, the tubes with resin coating displayed small-scale fragmentation in addition to buckling. For tubes subjected only to heat treatment, buckling occurred alongside tearing of the tube wall.

Figure 14 compares the fracture surfaces for tubes subjected to annealing only, resin coating only, and both resin coating and annealing. In tubes treated solely with annealing, a predominantly brittle fracture mode is evident. On the other hand, tubes treated solely with resin coating exhibit a propensity for a hackle pattern in PLA and a brittle fracture mode in the resin.

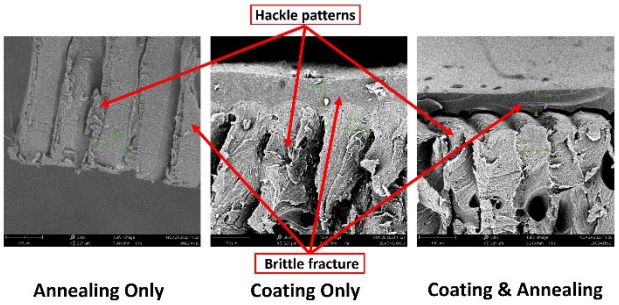

Fig. 14: The fracture surface affected by resin coating and heat treatment.

4. Conclusion

This study investigates the potential of resin coating and annealing to enhance the crashworthiness performance of TWMCS polymer 3D-printed tubes. The application of resin coating significantly improved crashworthiness performance, as evidenced by a substantial 41% increase in SEA value. Similarly, a marked improvement of 65% was observed in the MCF.

Attaining optimal SEA values was achieved by subjecting the specimens to an annealing process at 80°C, with annealing durations ranging from 40 to 120 minutes. The combined application of resin coating and annealing leads to a 57% increase in SEA compared to specimens without either treatment. The finding suggests that attaining optimum CFE values necessitates heat treatment at 80°C, with treatment durations varying between 70 and 120 minutes. As a result, the average CFE of the resin-coated and heat-treated tubes underwent a reduction of approximately 14%.

Future research directions include compatibility studies to ensure seamless integration of AM parts with existing materials in transportation systems. Additionally, exploring 3D-printed FDM-based material joints using both mechanical and adhesive techniques presents a compelling avenue for investigation.

Acknowledgements

This research is funded by the Directorate of Research and Development, Universitas Indonesia. The authors also acknowledge the facilities, scientific and technical support from Propellant and Quality Test Laboratories and Aeronautics Laboratories Rumpin, National Research and Innovation Agency through E-Layanan Sains-BRIN.

References

1) T. Pang, G. Zheng, J. Fang, D. Ruan, and G. Sun, "Energy absorption mechanism of axially-varying thickness (avt) multicell thin-walled structures under

out-of-plane loading," *Eng Struct*, **196** (2019). doi:10.1016/j.engstruct.2019.04.074.

2) A. Alavi Nia, and M. Parsapour, "Comparative analysis of energy absorption capacity of simple and multi-cell thin-walled tubes with triangular, square, hexagonal and octagonal sections," *Thin-Walled Structures*, **74** 155–165 (2014). doi:10.1016/j.tws.2013.10.005.
3) M. Haolei, X. Jiang, Z. Jun, and F. Zhenyu, "Experimental researches on failure and energy absorption of composite laminated thin-walled structures," *J Compos Mater*, **54** (*27*) 4253–4268 (2020). doi:10.1177/0021998320928135.
4) Y. Liu, J. Wang, R. Cai, J. Xiang, K. Wang, S. Yao, and Y. Peng, "Effects of loading rate and temperature on crushing behaviors of 3d printed multi-cell composite tubes," *Thin-Walled Structures*, **182** (2023). doi:10.1016/j.tws.2022.110311.
5) K. Wang, Y. Liu, J. Wang, J. Xiang, S. Yao, and Y. Peng, "On crashworthiness behaviors of 3d printed multi-cell filled thin-walled structures," *Eng Struct*, **254** (2022). doi:10.1016/j.engstruct.2022.113907.
6) D. Hidayat, J. Istiyanto, J.D. Nabilah, R. Ardiansyah, S.A. Saptari, F. Kurniawan, and D.A. Sumarsono, "Experimental investigation on axial quasi-static crushing of Al/PLA hybrid tubes," in: J Phys Conf Ser, Institute of Physics, 2023. doi:10.1088/1742-6596/2551/1/012008.
7) H. Yang, H. Lei, G. Lu, Z. Zhang, X. Li, and Y. Liu, "Energy absorption and failure pattern of hybrid composite tubes under quasi-static axial compression," *Compos B Eng*, **198** (2020). doi:10.1016/j.compositesb.2020.108217.
8) D. Hidayat, R. Ardiansyah, A. Nurrohmad, R.A. Ramadhan, J. Istiyanto, F. Karina, R.S. Aritonang, F. Kurniawan, and D.A. Sumarsono, "Experimental study on crashworthiness characteristics of composite hybrid tube utilise axial quasi-static crushing test," in: 2023: p. 020012. doi:10.1063/5.0181353.
9) X. Zhang, G. Cheng, and H. Zhang, "Theoretical prediction and numerical simulation of multi-cell square thin-walled structures," *Thin-Walled Structures*, **44** (*11*) 1185–1191 (2006). doi:10.1016/j.tws.2006.09.002.
10) M. Arjuna Putra Perdana, A. Hapid, A. Muharam, S. Kaleg, R. Ristiana, and A. Christantho Budiman, "Crashworthiness enhancement: the optimization of vehicle crash box performance by utilizing bionic-albuca spiralis thin-walled structure," *EVERGREEN Joint Journal of Novel Carbon Resource Sciences & Green Asia Strategy*, **10** (*03*) 1961–1967 (2023). doi:10.5109/7151754
11) D. Hidayat, J. Istiyanto, D.A. Sumarsono, F. Kurniawan, R. Ardiansyah, F.A. Wandono, and A. Nugroho, "Investigation on the crashworthiness performance of thin-walled multi-cell pla 3d-printed tubes: a multi-parameter analysis," *Designs (Basel)*, **7** (*5*) 108 (2023). doi:10.3390/designs7050108.
12) K. Wang, R. Cai, Z. Zhang, J. Liu, S. Ahzi, Y. Peng, and Y. Rao, "Compressive behaviors of 3d printed polypropylene-based composites at low and high strain rates," *Polym Test*, **103** (2021). doi:10.1016/j.polymertesting.2021.107321.
13) D. Hidayat, A. Nurrohmad, A. Nugroho, and L.R. Isna, "Experimental investigation on crashworthiness characteristics of e-glass-lycal composite tube and local product aluminum tube using quasi-static crushing test," in: AIP Conf Proc, 2020. doi:10.1063/5.0002313.
14) C.W. Isaac, and F. Duddeck, "Current trends in additively manufactured (3d printed) energy absorbing structures for crashworthiness application–a review," *Virtual Phys Prototyp*, **17** (*4*) 1058–1101 (2022). doi:10.1080/17452759.2022.2074698.
15) M.M. Ganganallimath, K. Vizayakumar, and U.M. Bhushi, "Comparative study of conventional wood-pattern with 3d-print abs-pattern to enhance quality of castings," *EVERGREEN Joint Journal of Novel Carbon Resource Sciences & Green Asia Strategy*, **10**(2) 1053–1060 (2023). doi:10.5109/6793662
16) B. Rusdyanto, F. Imaduddin, and D. Ariawan, "The tensile properties of recycled polypropylene filament (rpp) as 3d printing material," *Evergreen*, **10**(1) 489–495 (2023). doi:10.5109/6782152
17) S. Singh, L. Nagdeve, H. Kumar, and K. Dhakar, "Rice straw based natural fiber reinforced polymer for sustainable bio-composites: a systematic review," *Evergreen*, **10**(2) 1041–1052 (2023). doi:10.5109/6793661
18) J. Torres, J. Cotelo, J. Karl, and A.P. Gordon, "Mechanical property optimization of fdm pla in shear with multiple objectives," *JOM*, **67** (*5*) 1183–1193 (2015). doi:10.1007/s11837-015-1367-y.
19) I. Gibson, D. Rosen, and B. Stucker, "Additive Manufacturing Technologies 3D Printing, Rapid Prototyping, and Direct Digital Manufacturing Second Edition," n.d.
20) K.R. Hart, R.M. Dunn, J.M. Sietins, C.M. Hofmeister Mock, M.E. Mackay, and E.D. Wetzel, "Increased fracture toughness of additively manufactured amorphous thermoplastics via thermal annealing," *Polymer (Guildf)*, **144** 192–204 (2018). doi:10.1016/j.polymer.2018.04.024.
21) H.-C. Kim, D.-Y. Kim, J.-E. Lee, and K. Park, "Improvement of mechanical properties and surface finish of 3d-printed polylactic acid parts by constrained remelting," *Adv Mater Lett*, **8** (*12*) 1199–1203 (2017). doi:10.5185/amlett.2017.1686.
22) "Effects of coating on the fatigue endurance of fdm lattice structures," (n.d.).
23) M. Marian, D.F. Zambrano, B. Rothammer, V. Waltenberger, G. Boidi, A. Krapf, B. Merle, J. Stampfl, A. Rosenkranz, C. Gachot, and P.G. Grützmacher, "Combining multi-scale surface

texturing and dlc coatings for improved tribological performance of 3d printed polymers," *Surf Coat Technol*, **466** (2023). doi:10.1016/j.surfcoat.2023.129682.

24) H. Juliano, F. Gapsari, H. Izzuddin, T. Sudiro, K.Y. Phatama, W.P. Sukmajaya, Zuliantoni, T.M. Putri, and A.M. Sulaiman, "HA/zro2coating on cocr alloy using flame thermal spray," *Evergreen*, **9** (*2*) 254–261 (2022). doi:10.5109/4793632.
25) Y. Yang, W. Cao, Z. Wang, J. Li, and Y. Zhang, "Variation of mechanical properties and ballistic performance of fabric prepreg after resin coating processing," *Compos Struct*, **321** (2023). doi:10.1016/j.compstruct.2023.117232.
26) K.R. Hart, R.M. Dunn, and E.D. Wetzel, "Increased fracture toughness of additively manufactured semi-crystalline thermoplastics via thermal annealing," *Polymer (Guildf)*, **211** (2020). doi:10.1016/j.polymer.2020.123091.
27) A. Szust, and G. Adamski, "Using thermal annealing and salt remelting to increase tensile properties of 3d fdm prints," *Eng Fail Anal*, **132** (2022). doi:10.1016/j.engfailanal.2021.105932.
28) S. Wickramasinghe, T. Do, and P. Tran, "FDM-based 3d printing of polymer and associated composite: a review on mechanical properties, defects and treatments," *Polymers (Basel)*, **12** (*7*) 1–42 (2020). doi:10.3390/polym12071529.
29) R.A. Wach, P. Wolszczak, and A. Adamus-Wlodarczyk, "Enhancement of mechanical properties of fdm-pla parts via thermal annealing," *Macromol Mater Eng*, **303** (*9*) (2018). doi:10.1002/mame.201800169.
30) S. Bhandari, R.A. Lopez-Anido, and D.J. Gardner, "Enhancing the interlayer tensile strength of 3d printed short carbon fiber reinforced petg and pla composites via annealing," *Addit Manuf*, **30** (2019). doi:10.1016/j.addma.2019.100922.
31) E.R. Fitzharris, I. Watt, D.W. Rosen, and M.L. Shofner, "Interlayer bonding improvement of material extrusion parts with polyphenylene sulfide using the taguchi method," *Addit Manuf*, **24** 287–297 (2018). doi:10.1016/j.addma.2018.10.003.
32) S. Hou, Q. Li, S. Long, X. Yang, and W. Li, "Multiobjective optimization of multi-cell sections for the crashworthiness design," *Int J Impact Eng*, **35** (*11*) 1355–1367 (2008). doi:10.1016/j.ijimpeng.2007.09.003.
33) T. Jwaid, H. De Meyer, A.H. Ismail, and B. De Baets, "Curved splicing of copulas," *Inf Sci (N Y)*, **556** 95–110 (2021). doi:10.1016/j.ins.2020.12.053.
34) T. Jwaid, R. Mesiar, and A. Haj Ismail, "A generalization of quasi-homogenous copulas," *Fuzzy Sets Syst*, **441** 310–320 (2022). doi:10.1016/j.fss.2021.09.021.
35) G. Taguchi, and M.S. Phadke, "QUALITY ENGINEERING THROUGH DESIGN OPTIMIZATION," 1984.
36) N. Weake, M. Pant, A. Sheoran, A. Haleem, and H. Kumar, "Optimising parameters of fused filament fabrication process to achieve optimum tensile strength using artificial neural network," *Evergreen*, **7** (*3*) 373–381 (2020). doi:10.5109/4068614.
37) M. Awi, and A. Sufian Abdullah, "A review on mechanical properties and response of fibre metal laminate under impact loading (experiment)," *EVERGREEN Joint Journal of Novel Carbon Resource Sciences & Green Asia Strategy*, **10**(1) 111–129 (2023). doi:10.5109/6781057
38) A. Chueca de Bruijn, G. Gómez-Gras, L. Fernández-Ruano, L. Farràs-Tasias, and M.A. Pérez, "Optimization of a combined thermal annealing and isostatic pressing process for mechanical and surface enhancement of ultem fdm parts using doehlert experimental designs," *J Manuf Process*, **85** 1096–1115 (2023). doi:10.1016/j.jmapro.2022.12.027.